Available online at www.sciencedirect.com
ScienceDirect
Journal of Power Sources 162 (2006) 415–425
JOURNAL OF POWER SOURCES
www.elsevier.com/locate/jpowsour

Cross-leakage flow between adjacent flow channels in PEM fuel cells

Toshihiko Kanezaki [1], Xianguo Li *, J.J. Baschuk

Department of Mechanical Engineering, University of Waterloo, 220 University Avenue West, Waterloo, Ontario, Canada N2L 3G1

Received 21 April 2006; received in revised form 12 July 2006; accepted 12 July 2006
Available online 1 September 2006

Abstract

In polymer electrolyte membrane (PEM) fuel cells, serpentine flow channels are used conventionally for effective water removal. The reactant flows along the flow channel with pressure decrease due to the frictional and minor losses as well as the reactant depletion because of electrochemical reactions in the cells. Because of the short distance between the adjacent flow channels, often in the order of 1 mm or smaller, the pressure gradient between the adjacent flow channels is very large, driving part of reactant to flow through the porous electrode backing layer (or the so-called gas diffusion layer)—this cross-leakage flow between adjacent flow channels in PEM fuel cells has been largely ignored in previous studies. In this study, the effect of cross-flow in an electrode backing layer has been investigated numerically by considering bipolar plates with single-channel serpentine flow field for both the anode and cathode side. It is found that a significant amount of reactant gas flows through the porous electrode structure, due to the pressure difference, and enters the next flow channel, in addition to a portion entering the catalyst layer for reaction. Therefore, mixing occurs between the relatively high concentration reactant stream following the flow channel and the relatively low reactant concentration stream going through the electrode. It is observed that the cross-leakage flow influences the reactant concentration at the interface between the electrode and the catalyst layer, hence the distribution of reaction rate or current density generated. In practice, this cross-leakage flow in the cathode helps drive the liquid water out of the electrode structure for effective water management, partially responsible for the good PEM fuel cell performance using the serpentine flow channels.

Keywords: PEM fuel cells; Serpentine flow channels; Bipolar plates; Cross-leakage flow; Porous electrode; Analysis and simulation

1. Introduction

Polymer electrolyte membrane (PEM) fuel cell has been considered one of the most promising alternative clean power generator for portable, mobile and stationary applications, because of its low to zero emission (at least at the point of use), its low-temperature operation, high power density, and fast start-up. However, significant technical challenges have to be resolved before wide spread commercialization can occur, including cost reduction and better performance (including reliability and durability) [1]. These technical challenges are very much related to the two critical issues of water and heat management for PEM fuel cells [1,2], that mandate the use of complex flow channels on the bipolar plates, such as the serpentine flow channels shown in Fig. 1 [3]. The parallel flow channels connected in series, as shown in Fig. 1, result in a very long flow path, typically in the order of meters, while the dimension of the channel cross-section is often in the order of 1 mm or smaller. This long flow path not only causes excessive pressure loss, hence the pumping power requirement especially for the cathode air stream, but also a high manufacturing cost [3].

In an effort to improve PEM fuel cell performance, many analyses, models and numerical simulations have been developed [4,5] for various transport phenomena and electrochemical kinetics to gain a better understanding and to develop strategies for optimal design and operation. For example, optimal catalyst layer composition and structure have been investigated [6], the effect of water flooding [7], CO poisoning and oxygen bleeding [8,9] have been studied. Two or three-dimensional numerical simulation have been under development with various degrees of simplification by various research groups. You and Liu [10], Hum and Li [11] and Chena et al. [12] developed two-dimensional, along-the-channel models to model the flow and transport in the gas channel and porous gas diffusion

* Corresponding author.
E-mail address: x6li@uwaterloo.ca (X. Li).
[1] Present address: Department of Mechanical Engineering Science, Kyushu University, Fukuoka, Japan.

0378-7753/$ – see front matter © 2006 Elsevier B.V. All rights reserved.
doi:10.1016/j.jpowsour.2006.07.023

Nomenclature

A_C	Flow channel cross-sectional area (m^2)
A_R	Fuel cell active area (m^2)
C	Concentration ($mol\,m^{-3}$)
$C_{i,m}$	Mean concentration of reactant species i in the flow channel ($mol\,m^{-3}$)
$C_{i,s}$	Surface concentration of reactant species i ($mol\,m^{-3}$)
d_h	Hydraulic diameter (m)
D	Diffusion coefficient ($m^2\,s^{-1}$)
F	Faraday constant ($C\,mol^{-1}$)
h_m	Mass transfer coefficient ($m\,s^{-1}$)
I	Current density ($A\,m^{-2}$)
k	Permeability of electrode backing layer (m^2)
l	The length of flow channel (m)
L	The length and width of the bipolar plate (m)
$\dot{m}$	Mass flow rate ($kg\,s^{-1}$)
M_i	Mole weight of i specie ($kg\,mol^{-1}$)
$\dot{N}_i$	Molar flow rate of i specie ($mol\,s^{-1}$)
$\dot{N}_i''$	Molar flux of i specie ($mol\,m^{-2}\,s^{-1}$)
P	Pressure (Pa)
ΔP	Pressure difference (Pa)
r_0	Radius of bending (m)
Re_h	Reynolds number with hydraulic diameter
S_a	Anode stoichiometry
S_c	Cathode stoichiometry
$\boldsymbol{u}$	Phase-average velocity vector ($m\,s^{-1}$)
u	Velocity in x direction ($m\,s^{-1}$)
v	Velocity in y direction ($m\,s^{-1}$)
V	Mean flow velocity in the flow channel ($m\,s^{-1}$)
w_i	Mass fraction of i specie
w_c	Width of flow channel (m)
w_d	Height of flow channel (m)
w_s	Width of flow channel support (m)

Greek letters

δ_e	Thickness of electrode backing layer (m)
ϕ	Porosity of electrode backing layer
μ	Viscosity of mixture (Pa s)
ρ	Density of mixture ($kg\,m^{-3}$)
ξ	Loss coefficient
ξ_f	Coefficient of friction loss
ξ_b	Coefficient of bending loss

layer in the PEM fuel cell. Jeng et al. [13] presented the two-dimensional model in the cross-section perpendicular to flow channels to model the mass transport in the porous gas diffusion layer in the PEM fuel cell. Um and Wang [14] and Hu et al. [15] developed three-dimensional model and discussed the difference in performance between the parallel and interdigitated flow channels. They reported that an interdigitated flow channels could enhance mass transport and improve the PEM fuel cell performance compared to a parallel flow channels due to forced convectional flow through the porous electrode structure (the so-called gas diffusion layer referred to earlier). Conventional computational fluid dynamics techniques have also been used for the simulation of reactant flow in the flow channels [16,17].

Almost all the modeling and simulation studies reported in literature are based on the symmetry consideration as shown in Fig. 2 to reduce the computational effort. The computational domain is limited to two half adjacent channels and the portion of cell in between [18]. Such a simplification might be considered reasonable for parallel flow channel layout shown in Fig. 2b, but in reality it is not acceptable for PEM fuel cells, especially when the conventional serpentine flow channels like the one shown in Fig. 1 are used. This is because the reactant flow in each of the parallel channels differs, and in the case of serpentine flow channels the reactant gas experiences a pressure drop and concentration change along the channel. In case of a single serpentine flow channel shown in Fig. 1, the channel cross-section is small, in the order of 1 mm × 1 mm or smaller, while the channel length is very long, in the order of meters. Then the pressure drop at the corresponding location between the adjacent channels (for example, A–A′ in Fig. 1a) would be substantial, significant pressure gradient is thus set up across the porous electrode, much larger than the pressure gradient along the channel direction, resulting in considerable cross-leakage flow between the adjacent channels as illustrated in Fig. 1b. This significant cross-leakage flow through the porous electrode, as evidenced by the experimental pressure loss measurement [18], has been neglected for most of the previous studies, and in fact this flow induces a strong convection in the electrode, bringing the reactant gas to the catalyst layer and remove the product water from the reaction sites and electrodes, in a way similar to the flow set up in an interdigitated flow channels, responsible for the better overall cell performance when using the serpentine flow channels. Therefore, this cross-leakage flow has significant influence on PEM fuel cell performance and cannot be neglected.

In this study, the cross-leakage flow through the electrode is investigated as a direct result of the pressure difference between the adjacent channels. To provide a better understanding of this flow feature, two flow situations are investigated: the cross-leakage flow between two adjacent channels and over many adjacent channels. As shown later in this study, the cross-channel leakage flow is not only significant, but it might even become dominant as compared to the amount of the flow remaining in the flow channels. The present single-phase analysis is most likely to be valid on the anode, where dryout occurs at high current density, and it is less likely that any liquid accumulation exists in the porous electrode structure. The analysis can also be valid for low humidity cathode cases as well.

2. Model formulation

A PEM fuel cell consists of four major components, which are the bipolar (or flow distribution) plate, electrode backing layer (also sometimes referred to as gas-diffusion layer), catalyst layer, and polymer electrolyte membrane. The gas flow channels are typically rectangular or square grooves machined on the bipolar plate that distribute reactant gas over the fuel

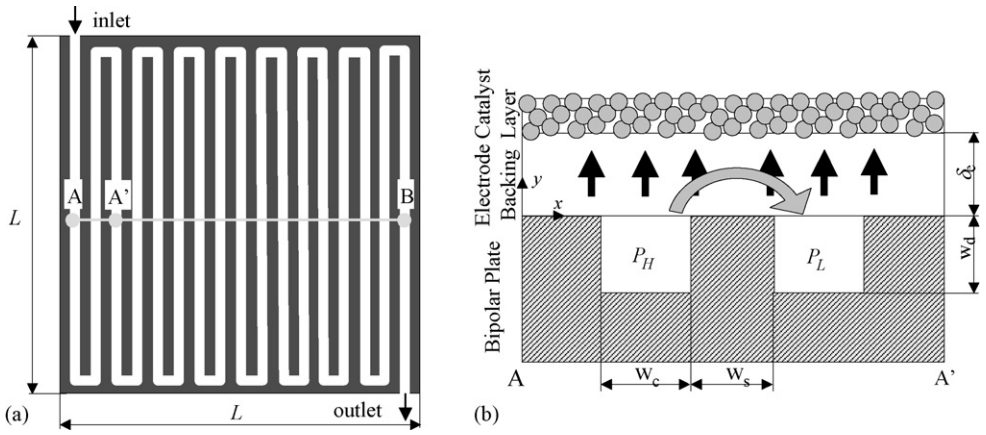

Fig. 1. Schematic of the bipolar plate with serpentine flow channel: (a) flow field layout; (b) the cross-sectional view of the bipolar plate and the porous electrode along the line A–A′, illustrating the cross-leakage flow between the two adjacent flow channels through the porous electrode structure, as presented by the thick arrow.

cell, and remove the product water out of the cell. The conventional bipolar plate with a single serpentine gas flow channel is considered in this study, as shown in Fig. 1a. The length and width of the bipolar plate are denoted by *L*. The reactant gas has a pressure drop along the channels. Therefore, there is significant local pressure differential between the adjacent channels due to the pressure loss along the flow channel. In this study, a two-dimensional approximation is considered in cross-section along the line A–A′ or A–B to model the cross-leakage flow through the electrode backing layer. The cross-sectional view of the bipolar plate and electrode along the line A–A′ is illustrated in Fig. 1b. Hydrogen is the reactant on the anode side, and is considered fully humidified. The reactant on the cathode side is oxygen with nitrogen because air is usually used. It is assumed that: (1) the gas mixtures behave as perfect gases, (2) the gas flow is under a steady state condition, (3) the electrode backing layers are considered to be isotropic porous media, (4) isothermal approximation is used as cooling is normally effective for PEM fuel cells, and (5) liquid water in the PEM fuel cell is not considered in this preliminary analysis.

After analyzing the cross-leakage flow between two adjacent flow channels, a further study is carried out for the cross-leakage

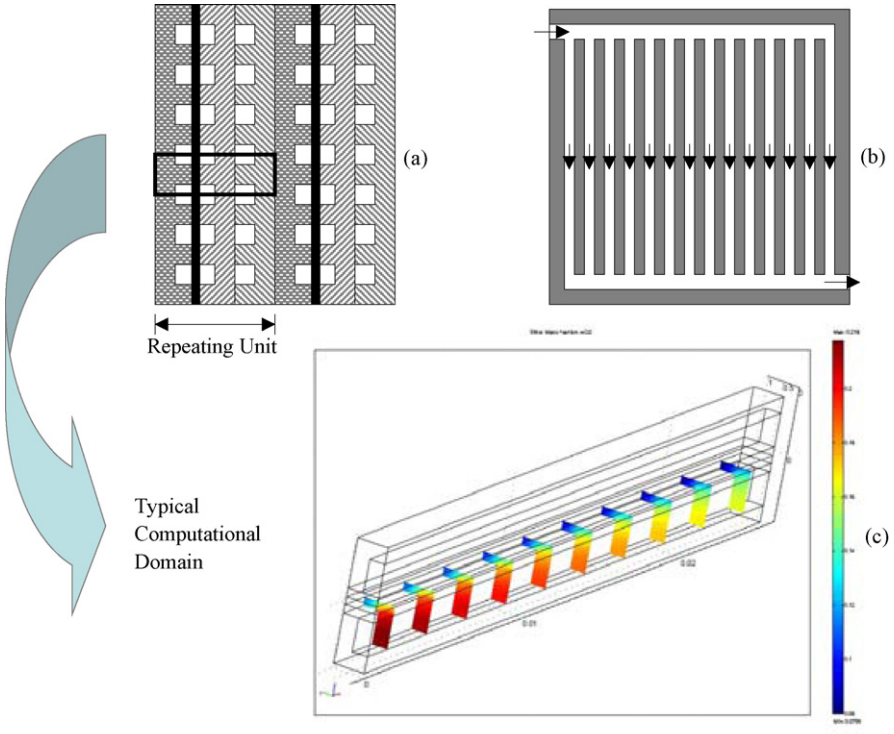

Fig. 2. A typical computational domain for CFD-based PEM fuel cell simulation. (a) A basic cell repeating unit in a PEM fuel cell stack, including a single cell sandwiched between two bipolar plates with flow channels and a cooling cell for thermal management; (b) a parallel flow channel layout; (c) a typical computational domain along the flow channel with symmetry condition at the middle of flow channels.

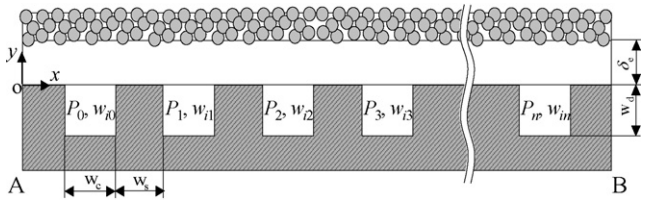

Fig. 3. The cross-sectional view of bipolar plate and electrode along the line A–B in Fig. 1a, illustrating the cross-leakage flow among many cascading flow channels.

flow among many adjacent flow channels. The latter is more realistic for PEM fuel cells, as shown in Fig. 3, which is essentially a cross-sectional view along the line A–B in Fig. 1a.

2.1. Governing equations in electrode backing layer

For the given physical problem shown in Fig. 1b, the flow field in the electrode backing layer is described by the conservation equations of mass, momentum, and species. The governing equation for the flow in the porous electrode is formulated by the volume-averaging technique [19]. The inertia term and the viscous term in the momentum equation is negligible because they are very small compared with the pressure term and Darcy's term [19]. The diffusive mass flux is modeled by using Fick's law of diffusion, since binary mixture is considered in the present analysis. Therefore, the conservation equations are

$$\text{Mass}: \quad \nabla \cdot (\phi \rho \mathbf{u}) = 0 \tag{1}$$

$$\text{Momentum}: \quad -\nabla P - \frac{\phi \mu}{k}\mathbf{u} = 0 \tag{2}$$

$$\text{Species}: \quad \nabla \cdot (\phi \rho w_i \mathbf{u}) - \nabla \cdot (\phi \rho D \nabla w_i) = 0 \tag{3}$$

$$\sum_i w_i = 1$$

where $\mathbf{u}$ is the phase-average velocity, ρ the density of the mixture, ϕ the porosity of the electrode, k the permeability of the electrode, μ the viscosity of the mixture, P the pressure, w_i the mass fraction of species i, and D is the effective diffusion coefficient. The Cartesian coordinate x and y are defined in Fig. 1b.

2.2. Pressure drop in the gas flow channel

Pressure drop arises due to the frictional loss and bending loss in the gas flow channel. The gas flow is assumed to be fully developed and laminar everywhere in the gas flow channel, because the entrance length is small compared to the total channel length as pointed out earlier. Then the pressure drop ΔP for the flow along the flow channel can be estimated as follows:

$$\Delta P = \frac{1}{2}\xi \rho V^2 \tag{4}$$

where V is the mean flow velocity in the flow channel, and ξ represents the loss coefficient. The loss coefficient ξ consists of the coefficients for frictional loss and bending loss. The frictional

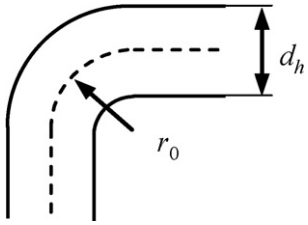

Fig. 4. Configuration of 90° bend.

loss coefficient ξ_f and the 90° bending loss coefficient ξ_b for a laminar flow and a square duct are given as follows [20]:

$$\xi = \xi_f + 2\xi_b \tag{5}$$

$$\xi_f = \frac{56.9}{Re_h} \cdot \frac{l}{d_h} \tag{6}$$

$$\xi_b = \frac{0.21}{(r_0/d_h)^{0.25}} + 50.4\frac{r_0}{d_h}\left(Re_h\sqrt{\frac{2r_0}{d_h}}\right)^{-2/3} \tag{7}$$

where l is the length of the flow channel as shown in Fig. 1a, d_h the hydraulic diameter, Re_h the Reynolds number using d_h, and r_0 is the radius of bending as shown in Fig. 4. The mean velocity V in the flow channel is determined from the Faraday's law of electrochemistry and the flow stoichiometry as follows:

$$\dot{N}_{H_2} = \frac{IA_R S_a}{2F}, \quad \dot{N}_{O_2} = \frac{IA_R S_c}{4F} \tag{8}$$

$$\dot{m} = \sum_i M_i \dot{N}_i \quad i: \text{ species (anode}: H_2,\ H_2O; \text{ cathode}: O_2,\ N_2,\ H_2O) \tag{9}$$

$$V = \frac{\dot{m}}{\rho A_C} \tag{10}$$

where I represents the current density of fuel cell, A_R the fuel cell active area, F the Faraday constant, S_a and S_c the anode and cathode stoichiometries, respectively, m the mass flow rate, M_i the mole weight of specie i, $\dot{N}_i$ the molar flow rate of specie i, and A_C denotes the flow channel cross-sectional area.

2.3. Boundary conditions

Several boundary conditions are necessary to solve the flow field in the electrode. At the interfaces between the electrode and the gas flow channels, the following boundary conditions are used,

$$P_n = P_o - n\,\Delta P_{A-A'} \tag{11}$$

$$w_{i,n} = w_{\text{specified}} \tag{12}$$

$$\left.\frac{\partial v}{\partial y}\right|_{y=0} = 0, \qquad u|_{y=0} = 0 \tag{13}$$

where P_n represents the pressure of nth flow channel from the inlet in cross-section along the line A–B, P_o the pressure of flow

channel at the point A in Fig. 1a, and $\Delta P_{A-A'}$, is the pressure difference between points A and A′ in Fig. 1a. The reactant concentration decreases along the flow channel. The reduction of reactant concentration is considered by following equations [1]:

$$h_m(C_{i,m} - C_{i,s}) = \dot{N}_i''$$
$$i: \text{reactant species (anode}: H_2, \text{ cathode}: O_2) \quad (14)$$

$$C_{i,m}(l) = (C_{i,m})_{in} - \frac{\dot{N}_i''}{w_d V} l \quad (15)$$

for low current densities, and

$$C_{i,m}(l) - C_{i,s}(l) = (C_{i,m} - C_{i,s})_{in} \exp\left(-\frac{h_m}{w_d V} l\right) \quad (16)$$

for high current densities. Where $\dot{N}_i''$ is the molar flux of species i, $C_{i,m}$ and $C_{i,s}$ the mean concentration of reactant species i in the flow channel and the electrode surface concentration of reactant species i, respectively, l the length of flow channel, w_d the height of flow channel, and h_m is the mass transfer coefficient, which is given by using the analogy with the heat transfer, for typical laminar flow in the fuel cell flow channels

$$Sh \equiv \frac{h_m d_h}{D} = 5.39 \quad \text{for uniform surface mass flux,}$$
$$\dot{N}_{i,s} = \text{const} \quad (17)$$

The mass fraction $w_{i,n}$ of each channels is calculated with the electrode surface concentration of the reactant $C_{i,s}$.

At the interfaces between the electrode and the gas flow channel supports, the following boundary conditions apply:

$$u|_{y=0} = 0 \quad (18)$$

$$\left.\frac{\partial w_i}{\partial y}\right|_{y=0} = 0 \quad (19)$$

The boundary conditions at the edges of the electrode are used as follows:

$$v|_{x=0,\,L} = 0 \quad (20)$$

$$\left.\frac{\partial w_i}{\partial x}\right|_{x=0,\,L} = 0 \quad (21)$$

The boundary condition at the interface between the electrode and the catalyst layer is approximated so that the current density I is constant. Hence, the boundary conditions are expressed as follows:

$$u|_{y=\delta_e} = 0 \quad (22)$$

$$\phi D \left.\frac{\partial C_{H_2}}{\partial y}\right|_{y=\delta_e} = -\frac{I}{2F}; \quad \text{for anode} \quad (23)$$

$$\phi D \left.\frac{\partial C_{O_2}}{\partial y}\right|_{y=\delta_e} = -\frac{I}{4F}; \quad \text{for cathode} \quad (24)$$

It should be pointed out that the above conditions at the interface between the electrode and the catalyst layer is very limiting, and a full consideration of the transport and reaction process would be needed to provide a more realistic boundary condition. This is avoided in this preliminary study to highlight the cross-leakage flow through the porous electrode structure.

3. Results and discussion

The governing equations are discretized by the finite-volume numerical technique, and the resulting set of algebraic equations is solved by tri-diagonal matrix solver. Both uniform and non-uniform grids have been used, and grid refinement study is carried out to achieve the grid-independent results. The design and operating conditions for the PEM fuel cell used for the present numerical simulation are given in Tables 1 and 2. The results are obtained for two flow situations: cross-leakage flow between two adjacent flow channels and among many cascading channels.

3.1. Cross-leakage flow between two adjacent flow channels

The cross-section along the line A–A′ as shown in Fig. 1 is considered first to model the cross-flow in the electrode backing layer when the current density of the cell is 0.6 A cm^{-2}. The average velocity in the flow channel is about 3.5 m s^{-1} for the anode and 11.8 m s^{-1} for the cathode.

Fig. 5 shows the streamline for the cross-leakage flow in the anode electrode. As expected, the streamline is from one flow channel to the next when there is pressure difference between the two channels as shown in Fig. 5a, whereas the flow is diffusional

Table 1
Operating parameters used in the present study

Cell temperature (K)	353
Anode inlet pressure (atm abs)	3
Anode gas mixture	H_2
Relative humidity (%)	100
H_2 stoichiometry	1.2
Cathode inlet pressure (atm abs)	3
Cathode gas mixture	21% O_2, 79% N_2
Relative humidity (%)	0
O_2 stoichiometry	2.0

Table 2
Design parameters used in the present study

Width of flow channel, w_c (m)	0.0011
Width of flow channel support, w_s (m)	0.0011
Height of flow channel, w_d (m)	0.0011
Radius of bending, r_0 (m)	0.0011
The length and width of the bipolar plate, L (m)	0.1
Fuel cell active area, A_R (m^2)	0.01
Thickness of electrode backing layer, δ_e (m)	2.5×10^{-4}
Porosity of electrode backing layer, ϕ	0.4
Permeability of electrode backing layer, k (m^2)	1.76×10^{-11} [a]

[a] Taken from Gurau et al. [21].

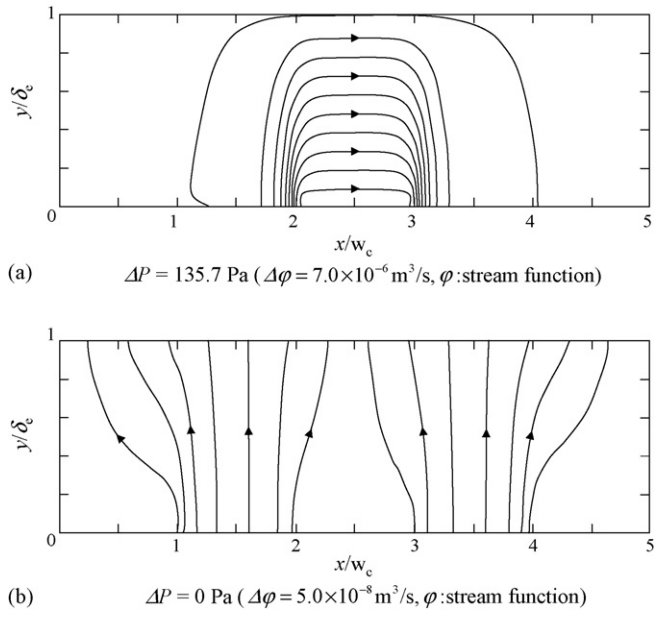

Fig. 5. (a and b) Streamline for the cross-leakage flow through the anode electrode.

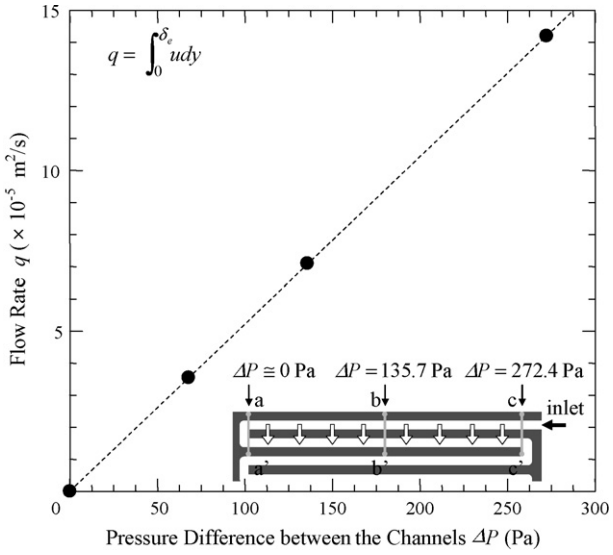

Fig. 7. Relationship between the flow rate for the cross-leakage flow through the anode and the pressure difference.

and directed towards the catalyst layer when the pressure difference vanishes, as seen in Fig. 5b. The velocity in the x direction at $x/w_c = 2.5$, corresponding to the middle of the channel support, is shown in Fig. 6. The velocity for the cross-leakage flow remains essentially constant throughout the electrode thickness, except near the two boundaries of the channel support and the catalyst layer. From the velocity distribution, the total flow rate for the cross-leakage flow through the electrode can be obtained by integrating along the electrode thickness, and Fig. 7 shows the relationship between the total flow rate q for the cross-leakage flow and the pressure difference ΔP, which changes along the flow channel for the two adjacent channels as indicated in the insert in Fig. 7. The flow rate q is almost proportional to the pressure difference ΔP, which is related to the channel length. Therefore, the flow rate through the electrode for each channel length can be calculated, which is $6.79 \times 10^{-6}\ m^3\ s^{-1}$. This is larger than the flow rate that remains in the gas channel ($4.26 \times 10^{-6}\ m^3\ s^{-1}$) under the same pressure difference. This result implies that a comparable amount of reactant gas flows through the electrode and along the channel to reach the same location in the next channel, because the same pressure difference yields much larger pressure gradient through the electrode than for the flow along the flow channel. This suggests that significant cross-flow through the electrode is observed, and cannot be neglected in such an analysis for PEM fuel cells.

A large quantity of the cross-flow affects the reactant concentration at the interface between the electrode and the cat-

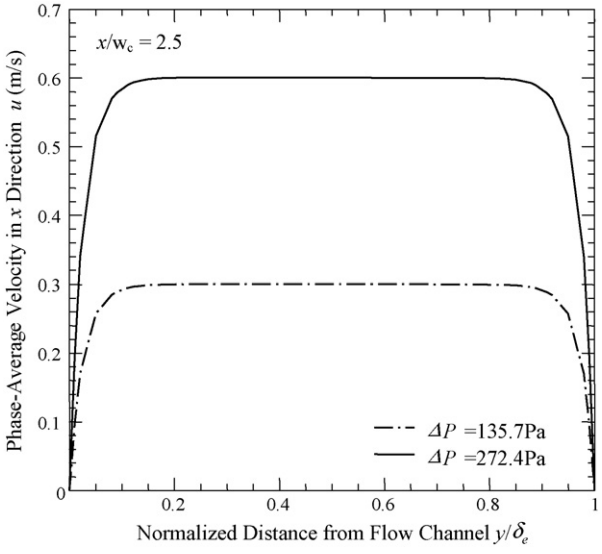

Fig. 6. Velocity distribution for the cross-leakage flow through the anode in x direction at $x/w_c = 2.5$, corresponding to the middle of the channel support region.

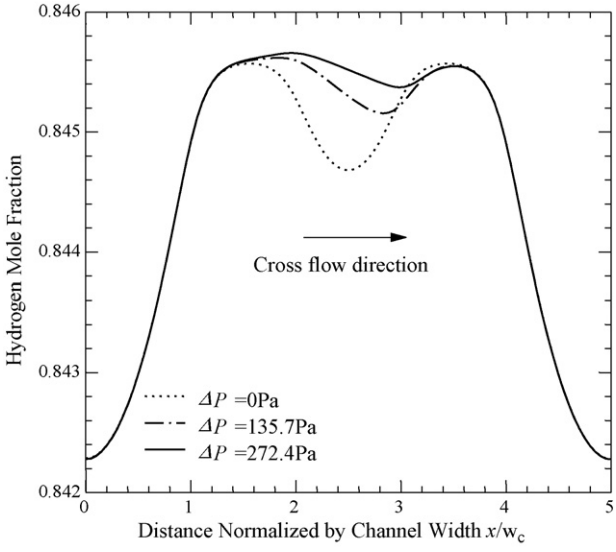

Fig. 8. Hydrogen mole fraction at the interface between the anode electrode and anode catalyst layer.

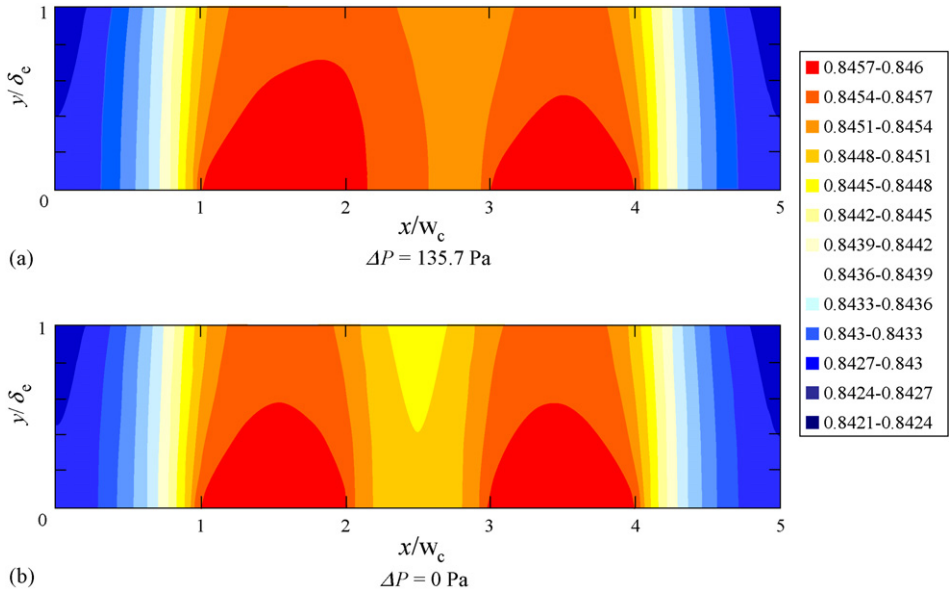

Fig. 9. Hydrogen molar fraction distribution over the entire anode electrode.

alyst layer. Fig. 8 shows the hydrogen mole fraction at the interface between the anode electrode and catalyst layer, and the hydrogen mole fraction over the entire electrode is given in Fig. 9. It is seen in Fig. 8 that the hydrogen concentration distribution is symmetric with respect to the middle of the channel support ($x/w_c = 2.5$) when the pressure difference is zero, since diffusion is the mechanism for mass transfer for this case. However, the cross-leakage flow set up by the pressure difference between the adjacent channels enhances considerably the hydrogen concentration at the catalyst layer, certainly beneficial for electrochemical reaction there. This is more evident in Fig. 9 for the region directly adjacent to the channel support where higher and more uniform hydrogen concentration is obtained with pressure difference. This effect becomes more significant as pressure difference is increased.

Fig. 10a shows the hydrogen concentration at the interface between the electrode and catalyst layer, while Fig. 10b shows the hydrogen concentration differential with respect to the case of $\Delta P = 0$ Pa. It is seen in Fig. 10a that the hydrogen concentration for the case of $\Delta P = 0$ is symmetrically distributed as noticed early for the hydrogen mole fraction, however, the peak value of the hydrogen concentration itself decreases in the downstream channel as a direct result of pressure drop and hydrogen consumption in the anode catalyst layer, and this decrease becomes larger as the value of ΔP is increased. On the other hand, the peak value in the upstream channel is slightly increased due to the convection current set up in the electrode structure. This trend is more vividly shown in Fig. 10b. It might be mentioned that in the present study, water flooding of the electrode has not been considered. Otherwise, the cross-leakage flow considered here can help remove the liquid water from the electrode structure, enhance reactant gas transport and improve the cell performance, just as forced convectional flow through the electrode enhances the performance with an interdigitated flow field [14,15].

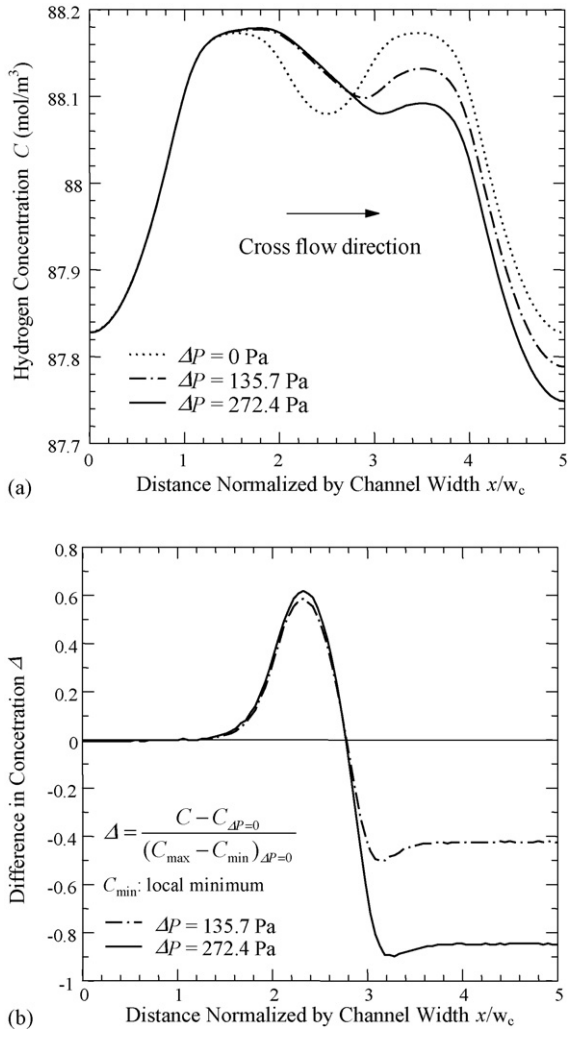

Fig. 10. Hydrogen concentration at the interface between the anode electrode and anode catalyst layer (a) with respect to the case without pressure difference (b).

Similar analysis has been carried out for the cathode flow, and the oxygen concentration at the interface between the cathode electrode and cathode catalyst layer as well as the oxygen concentration differential with respect to the case of $\Delta P = 0$ is shown in Fig. 11. It is seen that the base case with $\Delta P = 0$ is similar to the previous case for the anode hydrogen gas. Unlike the previous results for the anode gas, the oxygen concentration hardly changes as the pressure difference between the adjacent channels ΔP is increased. In fact, the oxygen concentration in the region corresponding to the channel support even becomes higher than the corresponding peak value of the oxygen concentration next to the flow channels for the case of $\Delta P = 0$. This is because the cathode gas is air, with relatively low oxygen concentration, and only oxygen diffuses to the cathode catalyst layer for electrochemical reaction, while the major species, nitrogen, is inert. As a result, the cross-leakage flow brings higher oxygen gas mixture in the flow channel to the significant portion of the electrode structure; this is more clearly shown in Fig. 12 for the contour plot for the oxygen mole fraction distribution. It is evident that the effect of the cross-leakage flow is much stronger for the cathode than for the anode, because the total cathode gas flow rate is much higher than the anode counterpart, due to the low oxygen content in the air and the much larger stoichiometry for the cathode (2 for the cathode versus 1.2 for the anode as shown in Table 1). The higher total cathode gas flow results in a higher pressure difference between the adjacent channels, thus a higher cross-leakage flow through the cathode electrode, as shown in Fig. 13 for the distribution of the phase-averaged velocity in the x direction at the middle of the channel support region. Clearly this cathode cross-flow velocity is much larger than the corresponding velocity in the anode shown in Fig. 6. Therefore, this much stronger cross-leakage flow through the cathode would be much more effective in water removal from the electrode structure, in addition to bringing higher oxygen concentration to the catalyst layer, thus enhancing the PEM fuel cell performance in practice. These results suggest the necessity of two-phase analysis in the next study on the

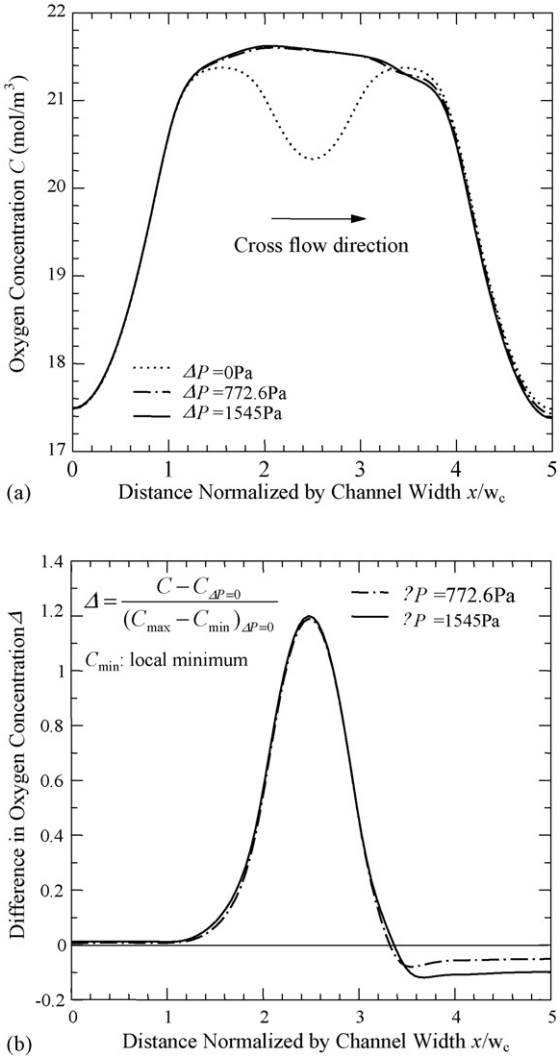

Fig. 11. Oxygen concentration at the interface between the cathode electrode and cathode catalyst layer (a) with respect to the case without pressure difference (b).

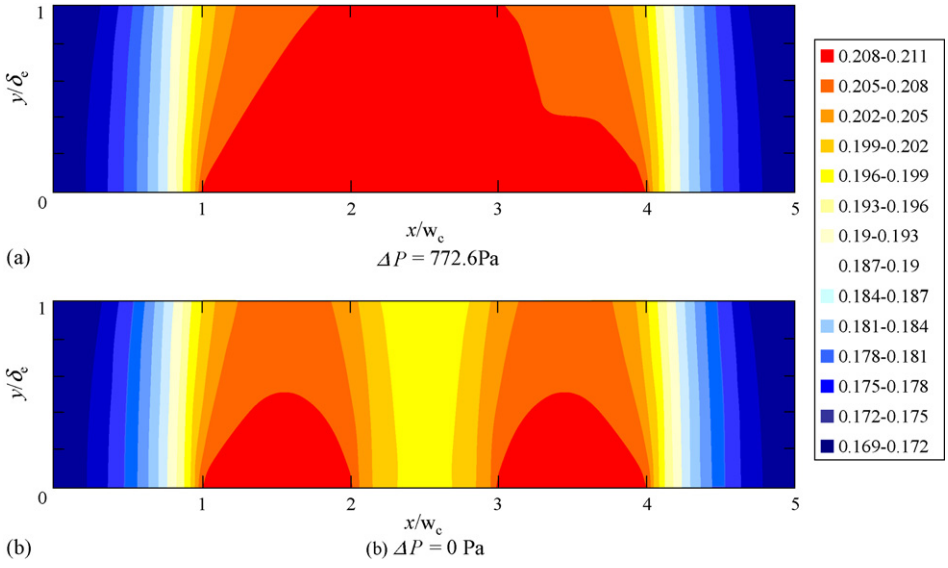

Fig. 12. Oxygen molar fraction distribution over the entire cathode electrode.

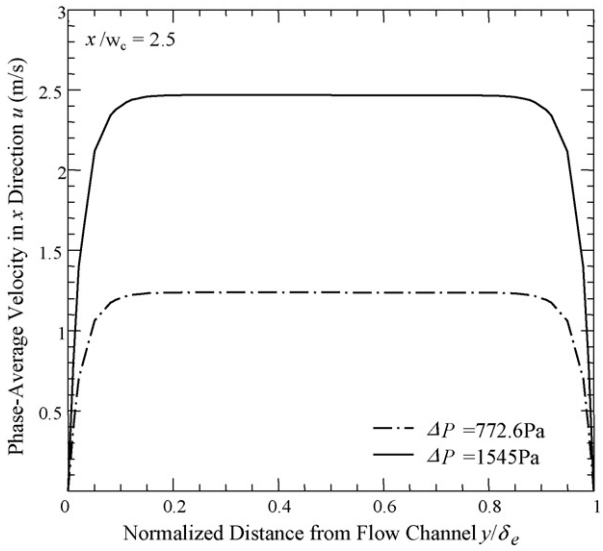

Fig. 13. Velocity distribution for the cross-leakage flow through the cathode in x direction at $x/w_c = 2.5$, corresponding to the middle of the channel support region.

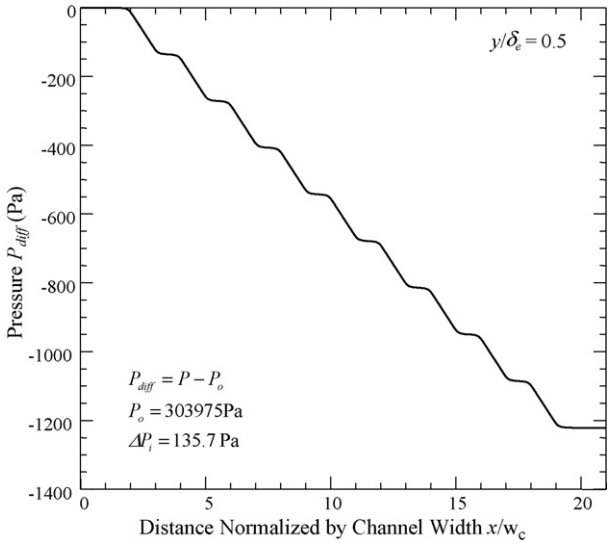

Fig. 14. Pressure distribution in anode electrode with similar pressure distribution for the cathode gas stream, the only difference is that the pressure drop between the adjacent flow channels DPI = 135.7 Pa for the anode gas stream and 772.6 Pa for the cathode gas stream.

effect of this cross-leakage flow much neglected in the previous studies.

3.2. Cross-leakage flow among many cascading flow channels

After analyzing the flow characteristics between two adjacent flow channels, we now turn our attention to the case of many flow channels adjacent to each other, as shown in Fig. 3 to investigate the more practical flow situation that is encountered in PEM fuel cells of practical size. With no loss of generality, we consider the situation of 10 cascading flow channels connected in series (the serpentine flow channels) for the average current density of 0.6 A cm^{-2}. The pressure distribution determined from the operating and design conditions given in Tables 1 and 2 is shown in Fig. 14 in the anode with similar distribution for the cathode, although cathode has much higher flow rate, hence a larger pressure drop between the successive channels ($\Delta P_i = 135.7$ Pa for the anode gas stream versus 772.6 Pa for the cathode gas stream). Fig. 15 shows the corresponding streamline pattern in the anode electrode, illustrating the cross-leakage flow from one flow channel to the next.

Fig. 16 presents the hydrogen concentration distribution at the interface between the anode electrode and anode catalyst layer showing the effect of the cross-leakage flow on the hydrogen concentration available at the catalyst layer. It is seen in Fig. 16a that the hydrogen mole fraction decreases from one channel to another in the flow direction, even for the case of no pressure drop, because of hydrogen consumption in the anode catalyst layer. The cross-leakage flow increases the hydrogen mole fraction available at the catalyst layer, especially for every region corresponding to the channel support area. However, Fig. 16b only shows the higher hydrogen concentration for the first couple of flow channel areas, then the hydrogen concentration corresponding to the flow with the pressure drop becomes smaller than the case without the pressure drop. This is because the pressure drop lowers the total pressure of the anode gas mixture, hence a lower total hydrogen concentration. This lower hydrogen concentration in the anode gas mixture is responsible for the gradual decrease in the total flow rate of the cross-leakage flow between the successive channels downstream, as shown in Fig. 17. Again the total flow rate through the electrode is comparable with the rate of the flow following the flow channels, as for the case for the two adjacent flow channels presented in the previous section.

The results for the cathode side are very similar to those for the anode side presented earlier. The only difference is that oxygen is only about 21% in the air, and with the higher stoichiometry of 2 for the oxygen as compared to 1.2 stoichiometry for the hydrogen on the anode, the total cathode stream has a much higher flow rate, thus a higher pressure drop between the successive channels, leading to almost an order of magnitude higher for the cross-leakage flow through the electrode, as shown in Fig. 18. For the results shown in Fig. 18, only eight flow channels are considered. This much stronger convection flow through the cathode electrode brings high oxygen concentration in the flow channel closer to the cathode catalyst layer.

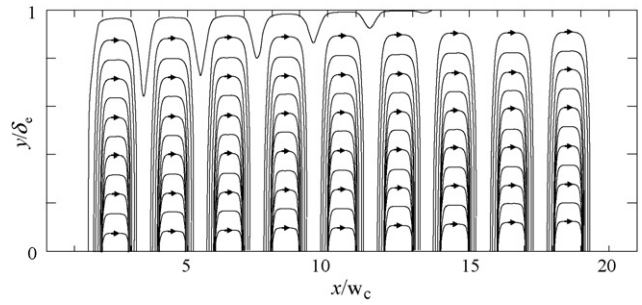

Fig. 15. Streamline in the anode electrode.

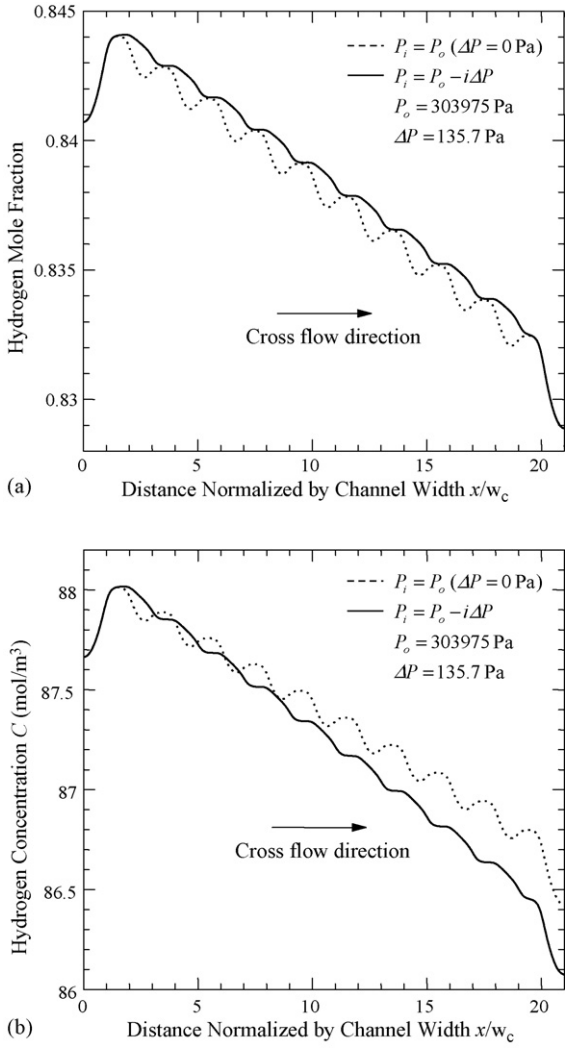

Fig. 16. Hydrogen distribution at the interface between the anode electrode and anode catalyst layer: (a) hydrogen mole fraction and (b) hydrogen concentration.

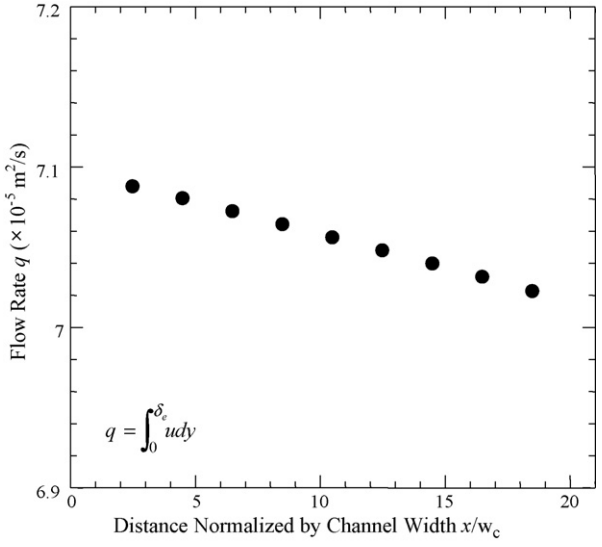

Fig. 17. The rate of the cross-leakage flow through the anode electrode corresponding to the x location at the middle of the channel support region (i.e., $x/w_c = 3.5, 5.5, 7.5, 9.5$, etc.).

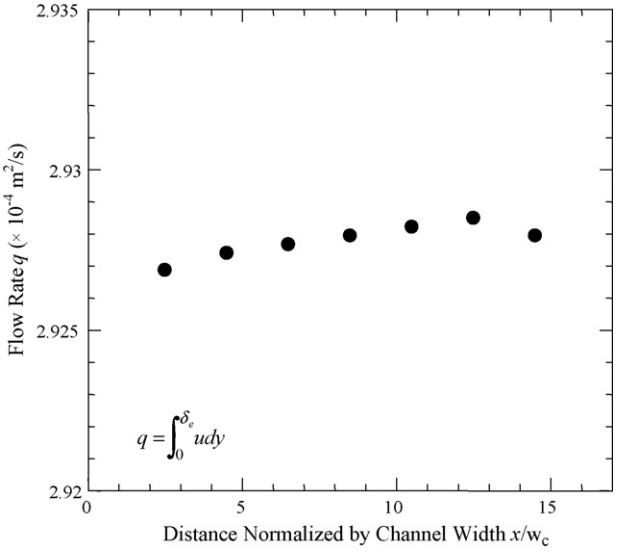

Fig. 18. The rate of the cross-leakage flow through the cathode electrode corresponding to the x location at the middle of the channel support region (i.e., $x/w_c = 3.5, 5.5, 7.5, 9.5$, etc.).

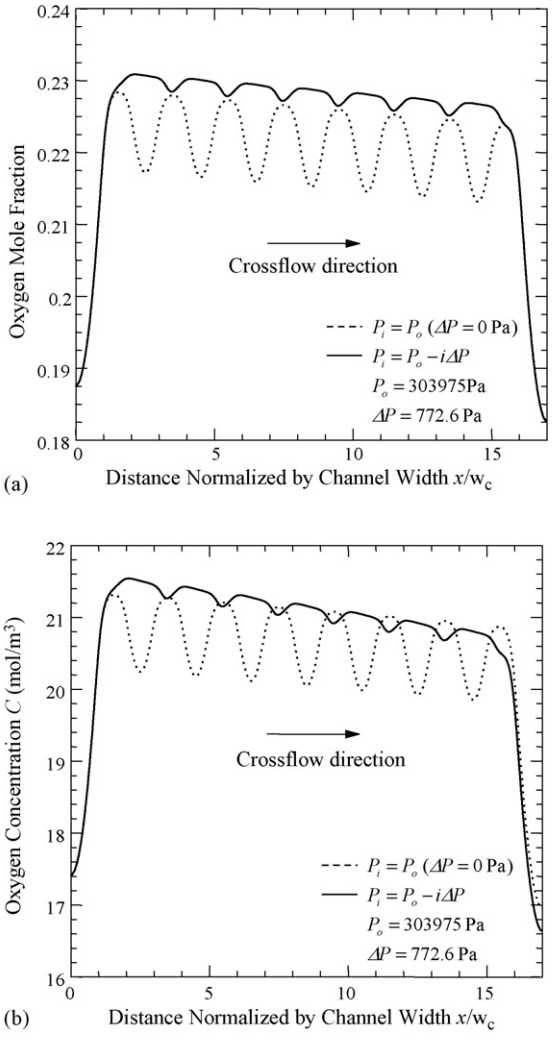

Fig. 19. Oxygen distribution at the interface between the cathode electrode and cathode catalyst layer: (a) oxygen mole fraction and (b) oxygen concentration.

Since this convection effect is in the same direction as the oxygen diffusion, the oxygen concentration, or mole fraction, near the catalyst layer can exceed their corresponding values in the flow channel, as shown in Fig. 19a and b, respectively. Therefore, this convection flow through the cathode electrode will be extremely beneficial for the removal of liquid water formed there, naturally leading to the next study by including both the three-dimensionality and the two-phase nature of the flow. Compared with the anode side shown in Fig. 16, the amount of oxygen concentration decrease between the successive downstream flow channels is much smaller, mainly because of the larger oxygen stoichiometry used.

4. Conclusions

This study presents a two-dimensional numerical simulation of the cross-leakage flow, through the PEM fuel cell electrode, between adjacent flow channels due to a pressure difference at the same locations among the successive channels by considering a single serpentine flow channel layout. It is found that a significant amount of the cross-leakage flow occurs, which is comparable with the amount of the flow that remains in the serpentine flow path for both the anode and cathode reactant gases. Because of the larger total cathode gas flow, the cross-flow rate for the cathode side (in the order of $10^{-5}\,m^3\,s^{-1}$) is almost an order of magnitude larger than the anode counterpart (in the order of $10^{-6}\,m^3\,s^{-1}$). The strong convection flow through the electrode structure is in general in the same direction as for the reactant diffusion to the catalyst layer, thus leading to a significantly higher concentration of the reactant in the catalyst layer, especially for the cathode side due to the much stronger leakage convection flow there. Consequently, this cross-leakage flow through the porous electrode can reduce concentration overpotential and help for the effective removal of liquid water in the electrode structure, thus explaining in part the well known experimental result of the good cell performance when using the serpentine flow channel design for PEM fuel cells.

References

[1] X. Li, Principles of Fuel Cells, Taylor & Francis, New York, 2006.
[2] A.S. Woodman, E.B. Anderson, K.D. Jayne, M.C. Kimble, Development of corrosion-resistant coatings for fuel cell bipolar plates, in: AESF SUR/FIN '99 Proceedings, vol. 6, 1999, pp. 21–24.
[3] X. Li, I. Sabir, Review of bipolar plates in PEM fuel cells, Int. J. Hydrogen Energy 142 (2004) 134–153.
[4] A. Biyikoglu, Review of proton exchange membrane fuel cell models, Int. J. Hydrogen Energy 30 (2005) 1181–1212.
[5] A.Z. Weber, J. Newman, Modeling transport in polymer–electrolyte fuel cells, Chem. Rev. 104 (2004) 4679–4726.
[6] C. Marr, X. Li, Composition and performance modeling of catalyst layer in a proton exchange membrane fuel cell, J. Power Sources 77 (1999) 17–27.
[7] J.J. Baschuk, X. Li, Modelling of polymer electrolyte membrane fuel cells with variable degrees of water flooding, J. Power Sources 86 (2000) 181–196.
[8] J.J. Baschuk, X. Li, Modelling CO poisoning and O2 bleeding in a PEM fuel cell anode, Int. J. Energy Res. 27 (2003) 1095–1116.
[9] J.J. Baschuk, X. Li, Mathematical model of a PEM fuel cell incorporating CO poisoning and O2 (air) bleeding, Int. J. Global Energy Issues 20 (3) (2003) 245–276.
[10] L. You, H. Liu, A two-phase flow and transport model for the cathode of PEM fuel cells, Int. J. Heat Mass Transfer 45 (2002) 2277–2287.
[11] B. Hum, X. Li, Two-dimensional analysis of PEM fuel cells, J. Appl. Electrochem. 34 (2004) 205–215.
[12] F. Chena, Y.-Z. Wen, H.-S. Chub, W.-M. Yan, C.-Y. Soong, Convenient two-dimensional model for design of fuel channels for proton exchange membrane fuel cells, J. Power Sources 128 (2004) 125–134.
[13] K.T. Jeng, S.F. Lee, G.F. Tsai, C.H. Wang, Oxygen mass transfer in PEM fuel cell gas diffusion layers, J. Power Sources 138 (2004) 41–50.
[14] S. Um, C.Y. Wang, Three-dimensional analysis of transport and electrochemical reactions in polymer electrolyte fuel cells, J. Power Sources 125 (2004) 40–51.
[15] G. Hu, J. Fan, S. Chen, Y. Liu, K. Cen, Three-dimensional numerical analysis of proton exchange membrane fuel cells (PEMFCs) with conventional and interdigitated flow fields, J. Power Sources 136 (2004) 1–9.
[16] E. Hontañón, M.J. Escudero, C. Bautista, P.L. García-Ybarra, L. Daza, Optimisation of flow-field in polymer electrolyte membrane fuel cells using computational fluid dynamics techniques, J. Power Sources 86 (2000) 363–368.
[17] A. Kumar, R.G. Reddy, Effect of channel dimensions and shape in the flow field distributor on the performance of PEM fuel cells, J. Power Sources 113 (2003) 11–18.
[18] X. Li, A comprehensive approach to the analysis of PEM fuel cells and stacks, Invited presentation at the Workshop on Computational Fuel Cell Dynamics, vol. III, Banff, Alberta, March 19–24, 2005.
[19] S. Whitaker, Flow in porous media. I. A theoretical derivation of Darcy's law, Transport Porous Media 1 (1986) 3–25.
[20] I.E. Idelchik, Handbook of Hydraulic Resistance, 3rd ed., CRC Press, Boca Ration, 1994.
[21] V. Gurau, H. Liu, S. Kakac, Two-dimensional model for proton exchange membrane fuel cells, AIChE J. 44 (1998) 2410–2422.